Report on Solving of Long-Wave Dynamics

Sulian Thual (CIMS), Andrew Majda (CIMS)

February 2013

Contents

1 Introduction

A broad perspective is to stochastise the skeleton model (Majda and Stechmann, 2009; Majda and Stechmann, 2011), such that it may account for irregular features of the MJO. One related issue is to design a suitable numerical method for solving. A split method is possible for this where one solves a long-wave equation using parabolic cylinder functions, and solves a master equation for a stochastic single-column skeleton model (cf meeting 02/06/13). In this report, we consider a numerical strategy to solve the long-wave equation.

Stochastic Skeleton Model: The stochastic skeleton model reads:

$$\begin{aligned}
&\partial_t u - yv - \partial_x \theta = 0 \\
&yu - \partial_y \theta = 0 \\
&\partial_t \theta - (\partial_x u + \partial_y v) = (\overline{H}\Delta a)\eta - s^\theta \\
&\partial_t q + \overline{Q}(\partial_x u + \partial_y v) = -(\overline{H}\Delta a)\eta + s^q \\
&\partial_t P(\eta) = [\lambda(\eta-1)P(\eta-1) - \lambda(\eta)P(\eta)] + [\mu(\eta+1)P(\eta+1) - \mu(\eta)P(\eta)]
\end{aligned} \tag{1}$$

with a periodic boundary condition on the equatorial belt of length L. This is derived from linearized primitive equations plus moisture budget projected on the first vertical baroclinic mode. Here u, v, θ, q are linearised around a RCE state at rest. The stochastic skeleton model includes a birth-death process accounting for intermittent bursts on the envelope of synoptic activity (that replaces the deterministic amplitude equation). Δa is constant, the random variable η is a positive integer, and λ and μ are transition rates of the birth-death process.

Long-Wave equation: In this report, we consider a numerical strategy to solve the long-wave equation of the stochastic skeleton model:

$$\begin{aligned} &(\partial_t + \varepsilon)u - yv - \partial_x\theta = 0 \\ &yu - \partial_y\theta = 0 \\ &(\partial_t + \varepsilon)\theta - (\partial_x u + \partial_y v) = S \end{aligned} \tag{2}$$

where S is here any given forcing, and where a dissipation rate ε has been added (assumed identical on u and θ in order to facilitate analytical treatment). There is also a periodic boundary condition on the equatorial belt of length L.

2 Parabolic Cylinder Functions

Basis of cylinder functions: Consider the parabolic cylinder functions (i.e. Hermite functions):

$$\phi_m(y) = \frac{H_m e^{-y^2/2}}{\sqrt{2^m m!\sqrt{\pi}}}, \text{ with Hermite polynomials } H_m(y) = (-1)^m e^{y^2}\frac{d^m}{dy^m}e^{-y^2} \tag{3}$$

that are defined for $m \geq 0$. The first Hermite polynomials read $H_o(y) = 1$, $H_1(y) = 2y$, $H_2(y) = 4y^2 - 2$. The cylinder functions satisfy the following recurrences:

$$L\_\phi_m = -\sqrt{2(m+1)}\phi_{m+1} \text{ and } L_+\phi_m = \sqrt{2m}\phi_{m-1}, \text{ with } L\pm = \frac{d}{dy} \pm y \tag{4}$$

$$\text{or similarly: } \sqrt{2}d_y\phi_m = -\sqrt{m+1}\phi_{m+1} + \sqrt{m}\phi_{m-1} \text{ and } \sqrt{2}y\phi_m = \sqrt{m+1}\phi_{m+1} + \sqrt{m}\phi_{m-1} \tag{5}$$

Define the inner product for any functions $g(y)$ and $h(y)$:

$$< g.h >= \int_{-\infty}^{+\infty} ghdy \tag{6}$$

For this inner product, the basis of cylinder functions is orthgonal and orthonormal:

$$< \phi_j.\phi_m >= \delta_{jm} \tag{7}$$

Spectral Approximation: Consider the truncated basis of cylinder functions $\phi_m(y)$, $0 \leq m \leq M-1$ (with M finite). Define the linear projector P, where for any function $f(x,y,t)$:

$$Pf = \sum_{m=0}^{M-1} f_m\phi_m(y), \text{ with } f_m(x,t) =< f.\phi_m > \tag{8}$$

Here (x,y,t) is the physical space, (x,m,t) is the spectral space, and the f_m are the spectral coefficients. The spectral approximation $f \approx Pf$ truncates f to the contribution of the M first cylinder functions. It can be used to solve a flow of functions $f(x,y,t)$, with operations involving dependency to y performed in spectral space. Using the recurrence properties of cylinder functions from equation 4, there is notably:

$$\partial_y f \approx P\partial_y Pf, \text{ with } P\partial_y Pf = \sum_{m=1}^{M-2}\frac{1}{\sqrt{2}}(f_{m+1}\sqrt{m+1} - f_{m-1}\sqrt{m})\phi_m(y) + \partial_y(f_0\phi_0 + f_{M-1}\phi_{M-1}) \tag{9}$$

$$yf \approx PyPf, \text{ with } PyPf = \sum_{m=1}^{M-2}\frac{1}{\sqrt{2}}(f_{m+1}\sqrt{m+1} + f_{m-1}\sqrt{m})\phi_m(y) + y(f_0\phi_0 + f_{M-1}\phi_{M-1}) \tag{10}$$

3 Equatorial Long-Waves

Equatorial Long-Waves: We follow the general method from Biello and Majda(2006, its appendix C-4 and C-5) to solve the long-wave equations 2 in the spectral space of cylinder functions. This spectral space is quite appropriate, because solving the flow is equivalent to solving independent systems for the evolution of Kelvin and Rossby waves. Those systems are simple transport equations with source term describing propagations of Riemann invariants.

Consider the the source term S, the Riemann invariant $Q = (u-\theta)/\sqrt{2}$, $R = (-u-\theta)/\sqrt{2}$, as well as their spectral coefficients, respectively S_m, Q_m and R_m.

Define the Kelvin wave amplitude $K = Q_0$. The evolution of $K(x,t)$ reads:

$$(\partial_t + \varepsilon)K + \partial_x K = -\frac{S_0}{\sqrt{2}} \tag{11}$$

Define the Rossby-m wave amplitude $\Omega_m = \sqrt{2}(\sqrt{m+1}\,Q_{m+1} + \sqrt{m}\,R_{m-1})$, for $1 \leq m \leq M-2$. The evolution of $\Omega_m(x,t)$ reads:

$$(\partial_t + \varepsilon)\Omega_m - \frac{\partial_x \Omega_m}{(2m+1)} = -\frac{2\sqrt{m(m+1)}}{2m+1}\left[\sqrt{m}\,S_{m+1} + \sqrt{m+1}\,S_{m-1}\right] \tag{12}$$

The Kelvin and Rossby waves considered here are non-dispersive. The Kelvin wave has a symetric meridional profile, no meridional velocity and no potential vorticity. The Rossby-m waves have meridional velocity and potential vorticity, with a meridional symetric (antisymetric) profile for m odd (even). For m large the meridional profiles of Rossby-m waves describe small scale structures confined to the equator. With the spectral approximation, the truncated flow can be reconstructed in physical space as follows:

$$u(x,y,t) = \frac{K}{\sqrt{2}}\phi_0 + \sum_{m=1}^{M-2}\frac{\Omega_m}{4}\left[\frac{\phi_{m+1}}{\sqrt{m+1}} - \frac{\phi_{m-1}}{\sqrt{m}}\right] \tag{13}$$

$$\theta(x,y,t) = -\frac{K}{\sqrt{2}}\phi_0 - \sum_{m=1}^{M-2}\frac{\Omega_m}{4}\left[\frac{\phi_{m+1}}{\sqrt{m+1}} + \frac{\phi_{m-1}}{\sqrt{m}}\right] \tag{14}$$

$$v(x,y,t) = \frac{S_1}{\sqrt{2}}\phi_0 + \sum_{m=1}^{M-2}\left[\partial_x\Omega_m + \sqrt{m+1}\,S_{m+1} - \sqrt{m}\,S_{m-1}\right]\frac{\phi_m}{\sqrt{2}(2m+1)} \tag{15}$$

4 Zonal Fourier Transform

Zonal Fourier transform: It is convenient to work with a Zonal Fourier Transform of the equations 11 and 12, that satisfy a periodic boundary condition on the equatorial belt of length L. For any function $f(x,t)$ defined on the zonal grid x_n,$0 \leq n \leq N-1$, with periodic boundary condition $f(0,t) = f(L,t)$, consider the Discrete Fourier Transform and Discrete Inverse Fourier Transform:

$$F(k,t) = \sum_{n=0}^{N-1} f(x_n,t)e^{-i2\pi kn/N} \text{ and } f(x_n,t) = \frac{1}{N}\sum_{k=0}^{N-1} F(k,t)e^{i2\pi kn/N} \tag{16}$$

where i is the complex number, and k is an integer satisfying $0 \leq k \leq N-1$. In practice we use the Fast Fourier Transorm (with N even), as in Majda and Stechmann (2011).

Solving either equation 11 or equation 12 consists in solving a transport equation with source term**:**

$$(\partial_t + \varepsilon)f + c\partial_x f = p \tag{17}$$

where f can be K or Ω_m. In Fourier space, assuming p constant from t to $t+dT$, the exact solutions are:

$$F(k,t+dT) = F(k,t)\exp(-\varepsilon t - 2\pi ikct) + \frac{P(k,t)}{\varepsilon + 2\pi ikc}\left(1 - \exp(-\varepsilon t - 2\pi ikct)\right) \tag{18}$$

$$F(0,t+dT) = F(0,t) + P(0,t)dT, \text{ for } k = 0 \text{ and } \varepsilon = 0 \tag{19}$$

where P is the Discrete Fourier Transform of p.

5 Gauss-Hermite Quadrature

Physical space: We follow the numerical method from Majda and Khouider (2001) to define a suitable physical space associated to the spectral space of cylinder functions. The long-wave equation 2 is solved in the spectral space of cylinder functions, which is a spectral method. Suppose now that the long-wave equation is further coupled to an evolution of the source term S that is best defined in physical space (e.g. as is the case for the stochastic skeleton model). To solve this flow, it is convenient to use a pseudo-spectral method, where the long-wave equation is solved in spectral space and the evolution of S is solved in physical space. For numerical solving, the physical space needs to be discrete.

Consider the spectral space (x,m,t), defined on the truncated basis of cylinder functions $\phi_m(y)$, $0 \leq m \leq M-1$. A suitable physical space is (x,y_k,t), where the y_k, $1 \leq k \leq M$ are the roots of the cylinder function ϕ_M (not included in the basis of cylinder functions). For $1 \leq k \leq M$, $\phi_M(y_k) = 0$. This gives a minimum number of discrete locations y_k where to simulate the flow in physical space.

Gauss-Hermite quadrature: The projection of any function $f(x,y_k,t)$ in spectral space (x,m,t) requires to compute the spectral coefficients $\overline{f}_m(x,t) =< f.\phi_m >$. The spectral coefficients can be approximated using the Gauss-Hermite quadrature:

$$f_m(x,t) \approx< f.\phi_m >_{GH} \tag{20}$$

where for any functions $g(y_k)$ and $h(y_k)$, we define the inner product:

$$< g.h >_{GH} = \sum_{k=1}^{M} g(y_k)h(y_k)\overline{H}_k, \text{ with } \overline{H}_k = \frac{1}{M(\phi_{M-1}(y_k))^2} \tag{21}$$

Note that the Gauss-Hermite quadrature is a more general method for approximating any integrals of kind $< g(y).e^{-y^2} > \approx < g(y_k).e^{-y_k^2} >_{GH}$.

To reconstruct the flow in physical space (x,y_k,t), define the linear projector P_{GH}, where for any function $f(x,y_k,t)$:

$$P_{GH}f = \sum_{m=0}^{M-1} f_m\phi_m(y_k), \text{ with } f_m(x,t) \approx< f.\phi_m >_{GH} \tag{22}$$

Note that the flow may as well be reconstructed in continuous physical space (x,y,t) using $f \approx Pf$.

Sensitivity to truncature order M: The truncature M of the cylinder function basis defines the number of solvable long-waves, as well as the number of discrete locations y_k in physical space. They are $M-1$ solvable long-waves (the Kelvin wave and $M-2$ Rossby waves). They are M discrete locations y_k in physical space. Figure 1 shows the spectral space and physical space for $M=3$: this configuration allows to solve K and Ω_1. Figure 2 shows the spectral space and physical space for $M=5$: this configuration allows to solve K and Ω_m, $1 \leq m \leq 3$ (notably $\Omega_2$has a meridionaly asymetric structure).

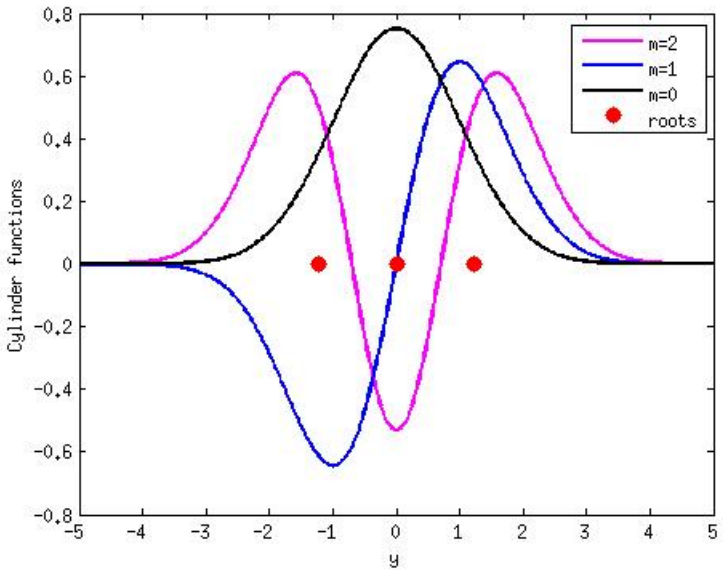

Figure 1: Spectral and physical space for $M = 3$: Plot of cylinder functions ϕ_m for $m = 0$ (black), $m = 1$ (blue), $m = 2$ (magenta). Roots y_k, $1 \leq k \leq M$ of ϕ_M (red dots). This truncature permits to solve the Kelvin wave K and Rossby wave Ω_1.

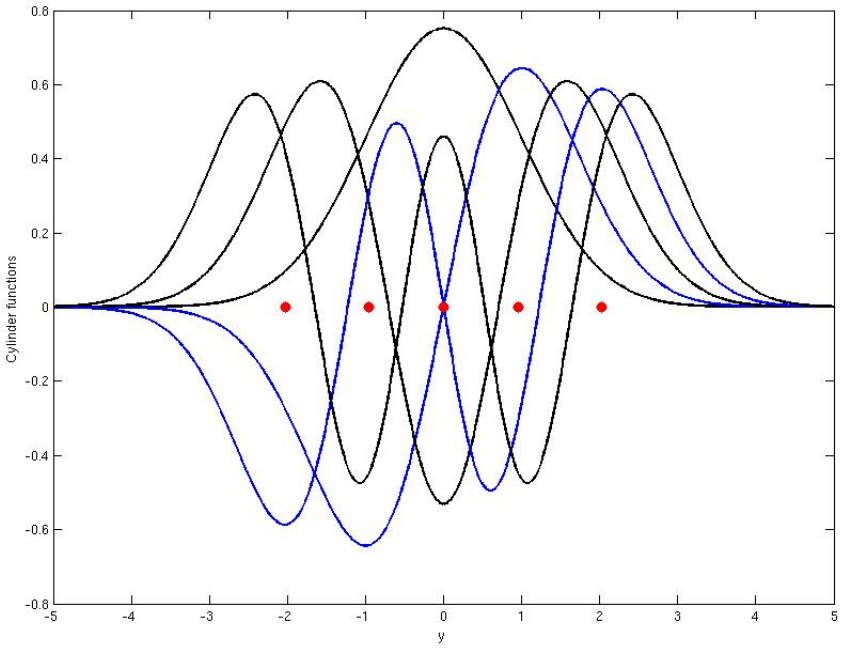

Figure 2: Spectral and physical space for $M = 5$: Plot of cylinder functions ϕ_m,$0 \leq m \leq M - 1$, for m even (black) and m odd (blue). Roots y_k, $1 \leq k \leq M$ of ϕ_M (red dots). This truncature permits to solve the Kelvin wave K and Rossby waves Ω_m, $1 \leq m \leq 3$.

6 Debug tests

Tranport Equation with source term: Consider equation 2 with a source term in given by:

$$S(x,y,t) = 2sin(kx)g(y)cos(\omega t) \tag{23}$$

where $g(y)$ is an arbitray function. To each equatorial wave corresponds an independent system (cf equations 11-12), which general form is a transport equation with source term:

$$\partial_t f + c\partial_x f = 2sin(kx)S_f cos(\omega t) \tag{24}$$

$$\text{with true solution } f(x,t) = \left(-\frac{cos(\omega t + kx)}{\omega + kc} + \frac{cos(\omega t - kx)}{\omega - kc} \right) S_f \tag{25}$$

where c is the phase speed, S_f is a constant arising from the meridional projection(s) of $g(y)$, and dissipation is omitted. To solve equation 24 we use the Zonal Fourier transform (cf section 4). Zonal and temporal steping is identical to Majda and Stechmann (2011), with 64 zonal grid points around the equatorial belt and a timestep $dT = dx/2$ in non-dimensional units. Initial conditions at $t = 0$ are from the true solution. Figure 3 shows solutions of equation 24 for $c = 1$, $S_f = 1$, k with wavenumber 1, and ω with period 20 days. The solutions with Zonal Fourier Transform are exact with respect to the true solution. In particular there is no CFL criterion, though for accuracy the timestep dT needs to small enough with respect to the period $1/\omega$ (not shown). For comparison, we also compute solutions with an approximated method of finite differences (of first order, with upward scheme for zonal propagations and Euler scheme in time), which is less accurate due to potential numerical dissipation or diffusion.

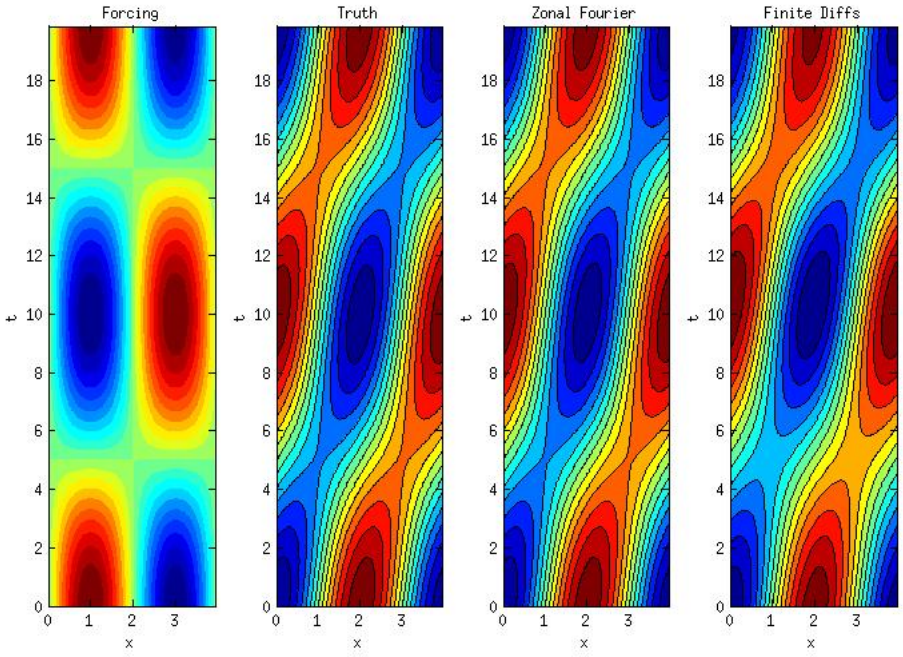

Figure 3: Solutions to transport equation with source term: Contour, as a function of x (10000 km) and t (days), of (a) source term p, (b) true solution f, (c) solution f computed from Zonal fourier transform method, and (d) f solved from finite differences method.

Meridional reconstruction 1: We consider an external forcing with simple meridional dependency:

$$S(x,y,t) = 2sin(kx)\phi_0 cos(\omega t) \tag{26}$$

that only forces a response on$K$ and Ω_1. We reconstruct the variables u, v, θ in physical space from the contribution of each equatorial wave.The true solution is:

$$u = \frac{cos(\omega t + kx)}{2(3\omega - k)}\left[\frac{\omega - 3k}{(\omega + k)}\phi_0 + \sqrt{2}\phi_2\right] + \frac{cos(\omega t - kx)}{2(3\omega + k)}\left[\frac{3k + \omega}{(k - \omega)}\phi_0 - \sqrt{2}\phi_2\right] \tag{27}$$

$$\theta = \frac{cos(\omega t + kx)}{2(3\omega - k)}\left[-\frac{5\omega + k}{(\omega + k)}\phi_0 - \sqrt{2}\phi_2\right] + \frac{cos(\omega t - kx)}{2(3\omega + k)}\left[\frac{k - 5\omega}{(k - \omega)}\phi_0 + \sqrt{2}\phi_2\right] \tag{28}$$

$$v = -\frac{4\phi_1}{3\sqrt{2}}\left[k\frac{sin(\omega t + kx)}{3\omega - k} + k\frac{sin(\omega t - kx)}{3\omega + k} + \frac{sin(kx)cos(\omega t)}{2}\right] \tag{29}$$

Figure 4 shows the true solution and simulated solution at a given timestep. They are in agreement. Note that the flow is solved using the physical space $(x, y_k t)$, but that we reconstruct in a more precise physical space (x, y, t) for the figure.

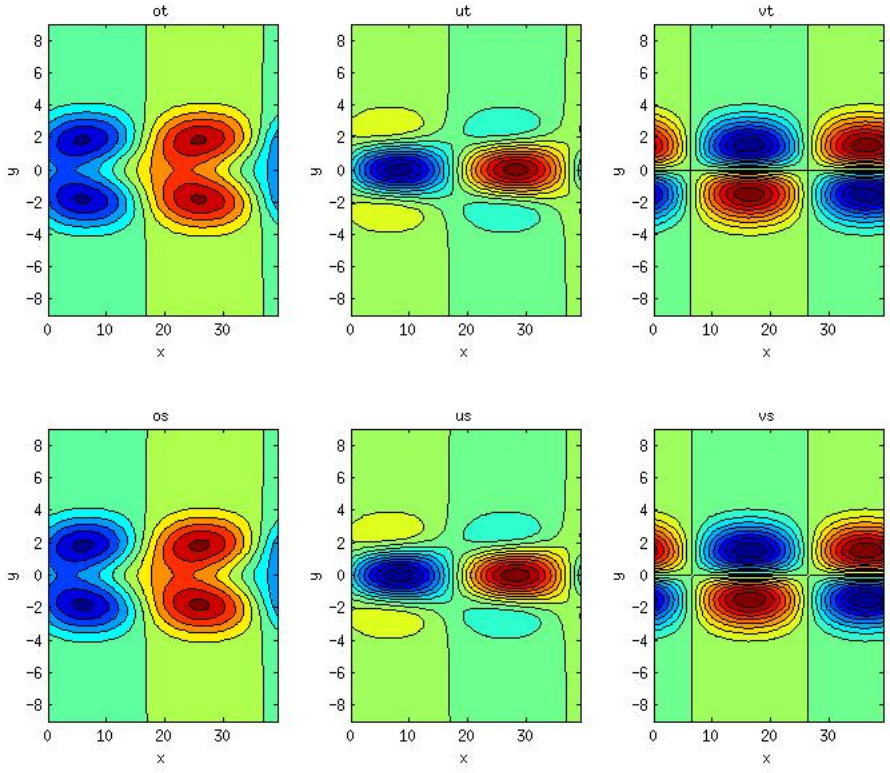

Figure 4: Solutions for source term on ϕ_0: Contour, as a function of x (1000 km) and y (1000km), of the true solution: (a) u, (b) θ, (c) v, and of the simulated solution: (d) u, (e) θ, (f) v. This is at $t = 17$ days.

Meridional reconstruction 2: We consider an external forcing with simple meridional dependency:

$$S(x, y, t) = 2sin(kx)\phi_1 cos(\omega t) \tag{30}$$

that only forces a response onΩ_2. We reconstruct the variables u, v, θ in physical space from the contribution of each equatorial wave. The true solution is:

$$u = \left(\frac{cos(\omega t + kx)}{5\omega - k} - \frac{cos(\omega t - kx)}{5\omega + k}\right)\left[\sqrt{\frac{3}{2}}\phi_3 - \frac{3}{2}\phi_1\right] \tag{31}$$

$$\theta = -\left(\frac{cos(\omega t + kx)}{5\omega - k} - \frac{cos(\omega t - kx)}{5\omega + k}\right)\left[\sqrt{\frac{3}{2}}\phi_3 + \frac{3}{2}\phi_1\right] \tag{32}$$

Figure 5 shows the true solution and simulated solution at a given timestep. They are in agreement.

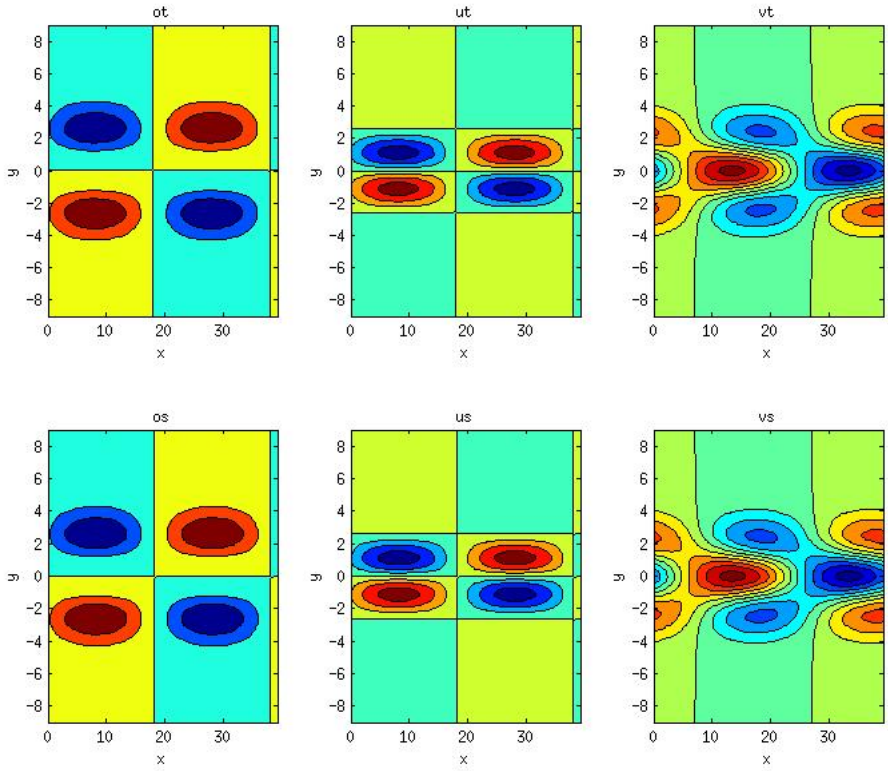

Figure 5: Solutions for source term on ϕ_1: Contour, as a function of x (1000 km) and y (1000km), of the true solution: (a) u, (b) θ, (c) v, and of the simulated solution: (d) u, (e) θ, (f) v. This is at $t = 17$ days.

Meridional reconstruction 3: We consider an external forcing with simple meridional dependency:

$$S(x, y, t) = 2sin(kx)\phi_2 cos(\omega t) \tag{33}$$

that only forces a response onΩ_1 and Ω_3. We reconstruct the variables u, v, θ in physical space from the contribution of each equatorial wave. The true solution is:

$$u = \left(\frac{cos(\omega t + kx)}{3\omega - k} - \frac{cos(\omega t - kx)}{3\omega + k}\right)\left[\frac{\phi_2}{2} - \frac{\phi_0}{\sqrt{2}}\right] + \left(\frac{cos(\omega t + kx)}{7\omega - k} - \frac{cos(\omega t - kx)}{7\omega + k}\right)\left[\sqrt{3}\phi_4 - \sqrt{6}\phi_2\right] \tag{34}$$

$$\theta = -\left(\frac{cos(\omega t + kx)}{3\omega - k} - \frac{cos(\omega t - kx)}{3\omega + k}\right)\left[\frac{\phi_2}{2} + \frac{\phi_0}{\sqrt{2}}\right] - \left(\frac{cos(\omega t + kx)}{7\omega - k} - \frac{cos(\omega t - kx)}{7\omega + k}\right)\left[\sqrt{3}\phi_4 + \sqrt{6}\phi_2\right] \tag{35}$$

$$v = v_1\frac{2}{3}\phi_1 + v_3\frac{4\sqrt{6}}{7}\phi_3 \tag{36}$$

$$v_1 = -k\frac{sin(\omega t + kx)}{3\omega - k} - k\frac{sin(\omega t - kx)}{3\omega + k} + +sin(kx)cos(\omega t) \tag{37}$$

$$v_3 = -k\frac{sin(\omega t + kx)}{7\omega - k} - k\frac{sin(\omega t - kx)}{7\omega + k} - \frac{sin(kx)cos(\omega t)}{4} \tag{38}$$

Figure 6 shows the true solution and simulated solution at a given timestep. They are in agreement.

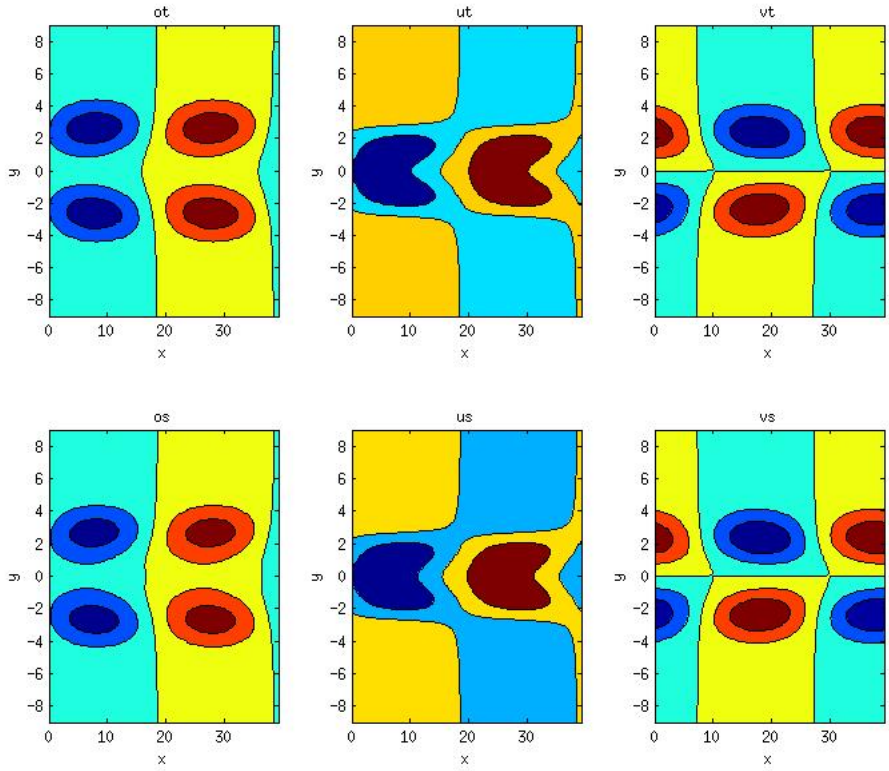

Figure 6: Solutions for source term on ϕ_2: Contour, as a function of x (1000 km) and y (1000km), of the true solution: (a) u, (b) θ, (c) v, and of the simulated solution: (d) u, (e) θ, (f) v. This is at $t = 17$ days.

Meridional reconstruction 4: We consider an external forcing with meridional dependency:

$$S(x, y, t) = 2sin(kx)exp(\lambda(y - \mu)^2)cos(\omega t) \tag{39}$$

which is off-equatorial, and were we choose $\lambda = 0.1$ and $\mu = 3$ in non-dimensional units. To solve the flow we consider a truncature to $M = 10$ (only the first $M - 2$ Rossby waves are considered). The true solution may be reconstructed using equation 25 for each equatorial wave (not shown). Figure 7 shows the true solution and simulated solution at a given timestep. They are in agreement.

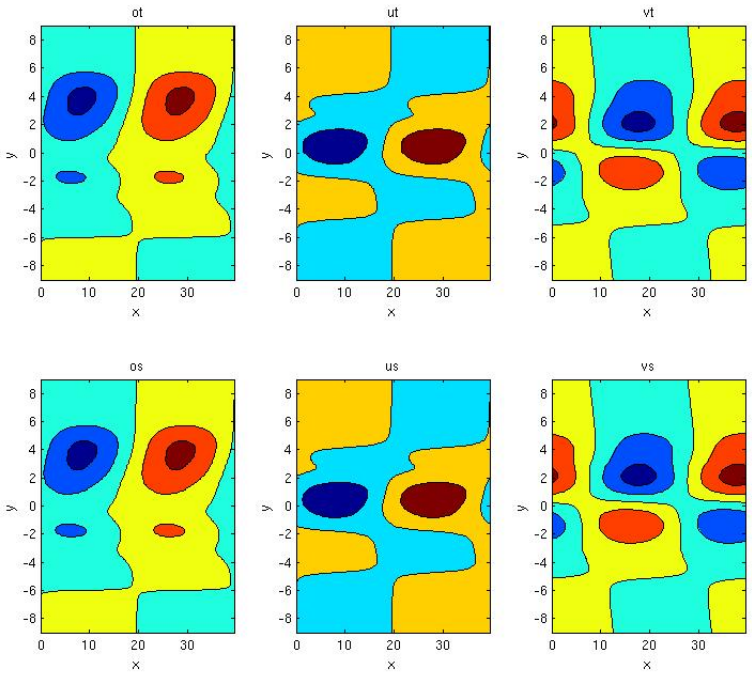

Figure 7: Solutions for off-equatorial source term: Contour, as a function of x (1000 km) and y (1000km), of the true solution: (a) u, (b) θ, (c) v, and of the simulated solution: (d) u, (e) θ, (f) v. This is at $t = 17$ days.

Further tests: All tests from this section were also performed for zonal wavenumber 2 and 3, and simulated solutions were in agreement with true solutions (not shown).

7 Summary of Results

We have considered a strategy to solve the long-wave equations in the stochastic skeleton model. Main results are as follow:

- The long-wave equations are easily solved in the spectral space of cylinder functions, as independent systems.
- To solve each system, the zonal Fourier transform leads to exact solution.
- For pseudo-spectral methods, a suitable discrete physical space is given by the Gauss-Hermite quadrature.

References

Biello, J. A. and Majda, A. J. (2006). Modulating synoptic scale convective activity and boundary layer dissipation in the IPESD models of the Madden-Julian oscillation. *Dynamics of Atmospheres and Oceans*, 42(1-4):152–215.

Majda, A. J. and Khouider, B. (2001). A numerical strategy for efficient modeling of the equatorial wave guide. *Proceedings of the National Academy of Sciences of the United States of America*, 98(4):1341–1346.

Majda, A. J. and Stechmann, S. N. (2009). The skeleton of tropical intraseasonal oscillations. *Proceedings of the National Academy of Sciences*, 106(21):8417–8422.

Majda, A. J. and Stechmann, S. N. (2011). Nonlinear dynamics and regional variations in the MJO skeleton. *Journal of the Atmospheric Sciences*, 68(12):3053–3071.